

Permeability Prediction in the South Georgia Rift Basin – Applications to CO₂ Storage and Regional Tectonics

Olusoga Martins Akintunde (✉ olusogamartins@gmail.com)

University of South Carolina College of Arts and Sciences <https://orcid.org/0000-0001-6711-2988>

Camelia C. Knapp

Oklahoma State University Stillwater

James H. Knapp

Oklahoma State University Stillwater

Research Article

Keywords: CO₂ storage, South Georgia Rift (SGR), geohydraulic properties

Posted Date: February 10th, 2021

DOI: <https://doi.org/10.21203/rs.3.rs-180571/v1>

License:  This work is licensed under a Creative Commons Attribution 4.0 International License.

[Read Full License](#)

1 **Permeability Prediction in the South Georgia Rift Basin – Applications to CO₂ Storage and**
2 **Regional Tectonics**

3

4 Olusoga M. Akintunde*, Camelia C. Knapp**, and James H. Knapp**

5 *Formerly University of South Carolina, Columbia, South Carolina

6 **Boone Pickens School of Geology, Oklahoma State University

7

8 **Acknowledgements and Disclaimer**

9 We thank John Shafer, Mike Waddell, Adrian Addison, Duke Brantley, Mark Evans, David
10 Heffner, Scott Howard, and Bill Clendenin for their contributions to this study. We also thank
11 Professor Manika Prasad of the Colorado School of Mines in Golden, Colorado, for access to
12 their Rock Physics Laboratory facilities. The thin sections that we used were provided by Dr.
13 James Rine of the Weatherford Laboratories. We acknowledge the helpful comments from our
14 anonymous reviewers. This material is based upon work supported by the United States
15 Department of Energy (DOE) under Award Number DE-FE0001965. This paper was prepared as
16 an account of work sponsored by an agency of the United States Government. Neither the United
17 States Government nor any agency thereof, nor any of their employees, make any warranty,
18 express or implied, or assume any legal liability or responsibility for the accuracy, completeness,
19 or usefulness of any information, apparatus, product, or process disclosed, or represents that its
20 use would not infringe privately owned rights. Reference herein to any specific commercial
21 product, process, or service by trade name, trademark, manufacturer, or otherwise does not
22 necessarily constitute or imply its endorsement, recommendation, or favoring by the United
23 States Government or any agency thereof.

24 **Abstract**

25 The lack of the permeability log data necessary to assess reservoir injectivity as well as aid in the
26 correlation and interpretation of existing porosity and resistivity logs for reservoir quality
27 characterization for potential CO₂ storage in the heterogenous and complex South Georgia Rift

28 (SGR) basin provides the motivation for this study. The focus was on the Triassic-Jurassic red
29 beds buried, entrenched beneath the Cretaceous-Cenozoic Coastal Plain sediments. Moreover,
30 the significant cost typically between \$10 M to \$100M associated with drilling and logging for in
31 situ permeability coupled with the limited resolution of existing core data further makes this
32 work necessary. The purpose is to relate, use the interpretation of the predicted permeability
33 distribution to assess feasibility for safe and long-term CO₂ sequestration. This study also intends
34 to establish the impacts of active and passive tectonism that has shaped and/or re-shaped the
35 evolution of the basin on the present-day permeability. A methodology was applied that utilizes
36 the pore space and geohydraulic properties of the reservoir from existing laboratory and well
37 data to produce a newly derived permeability log. It shows a non-uniform distribution with
38 depths possibly due to geologic changes in the confined and heterogeneous red beds. The derived
39 log displays characteristics consistent with observations from the porosity and resistivity logs.
40 The interpretation of these logs provides evidence for the presence of low permeable, tightly
41 cemented and compacted red beds. We conclude that the low permeability aided by the low
42 resistivity depicted in the red beds suggests increased confining stress and reduced injectivity,
43 and that the uncharacteristically low permeability reflects a deformed basin shaped with episodes
44 of uplift and erosion.

45 **Introduction**

46 Permeability is an important reservoir property that measures the ability of a rock to allow fluid
47 to pass through. It is a function of the pore space and pore connectivity within a rock (Mavko et
48 al., 2003). Its pore space property enables it to have a direct, linear relationship with porosity. A
49 rock with high porosity would typically exhibit high permeability so long as it is characterized
50 by large and uniformly rounded grains. However, poor sorting and presence of fine grain

51 materials can reduce permeability even if the porosity is high. Porosity is heavily influenced by
52 the rock's pore space and grain size distribution, while permeability is controlled by a
53 combination of these factors as well as by other subsurface or near surface fluid flow properties
54 such as tortuosity, pore shape and pore throats.

55 Permeability as a rock property complements porosity for the purpose of assessing reservoir
56 quality either for fluid injection involving CO₂ storage or for oil and gas exploration and
57 development. Its importance to the evaluation of the suitability of the confined and porous red
58 beds formations of the SGR basin for safe and permanent geologic CO₂ sequestration makes it of
59 great interest to this study.

60 The SGR basin was formed about 215 – 175 Ma through the breakup of Pangaea and opening of
61 the Atlantic. It is believed to be the largest and probably the most geologically complex
62 Mesozoic graben of the Eastern North American Passive Margin (McBride et al., 1989; and
63 Chowns and Williams, 1983). As shown in Figure 1, it covers an area of about 100,000 km²
64 encompassing South Carolina, Georgia, Alabama, and parts of Florida (Chowns and Williams,
65 1983). The basin fills consist of basalts, diabase sills and red beds. Extrusion of the basalt and
66 intrusion of the diabase sills followed the post rifting events that occurred during the Jurassic
67 (Chowns and Williams, 1983; Ghon, 1983; Ghon et al., 1983; and Olsen et al., 1991). The red
68 beds were formed through sediment deposition that accompanied the formation of the basin in
69 late Triassic. Studies by Heffner et al. (2012), Akintunde et al. (2013a), and McBride et al.
70 (1989) show the SGR basin fills to be overlain by the Cretaceous-Cenozoic sediments.

71 This study focuses on the red beds found in the Norris Lightsey #1 well, in Northwest Colleton
72 County, South Carolina (Figure 1). The Norris Lightsey #1 was a wild cat well drilled in the

73 early 1980s to explore for hydrocarbons. It is also one of the very few wells in Southern South
74 Carolina with significant penetration of the Triassic red beds, covering a depth of about 4,000 m
75 and penetrating over 3,100 m of Triassic red beds. The lithology of the Norris Lightsey red beds
76 consists of fine grained sandstones that are mixed with siltstone, conglomerate and mudstone
77 (Figure 2). Geological characterization of these red beds for optimum reservoir quality
78 assessment for safe and permanent CO₂ storage will require the interpretation and correlation of
79 a combination of relevant well logs. Core scale laboratory data are of limited resolution and are
80 characterized by coarse sampling at depth. On the other hand, well logs offer fine spatial
81 sampling and continuity that are absolutely essential for comprehensive and uncompromising
82 assessment of the state and suitability of a target reservoir for CO₂ storage. Unlike core scaled
83 data, knowledge of reservoir permeability at in situ conditions is important to dynamic reservoir
84 modeling for better understanding and accurate prediction of the distribution of fluid flow for
85 injection optimization and management. Unfortunately for the study location, there is no log of
86 permeability changes at depth to either assess the suitability of the porous red beds for injectivity
87 or correlate with available porosity and resistivity logs to aid site characterization. This lack of a
88 permeability log, especially at reservoir depths not sampled by the available core laboratory data
89 (Table 1), provides the motivation for this study.

90 **Objectives**

91 In evaluating subsurface suitability for CO₂ storage in a heterogeneous reservoir such as the
92 confined red beds formations encountered in this study area, three questions are important to the
93 interpretation of permeability. How does the permeability change with depth? What do the
94 observed changes reveal about the state of the reservoir for potential CO₂ storage? Do the depth-
95 varying permeability changes exhibit the same behavior as porosities at same depth intervals? A

106 permeability log because of its continuity within the subsurface meets the optimum resolution
107 required to better quantify, understand and interpret depth dependent permeability changes as
108 these relate to the above questions. Moreover, laboratory derived core scale porosity and
109 permeability measurements (Table 1) are limited in resolution, while porosity and permeability
110 information from wells logs provide continuous coverage for reservoir quality assessment. Core
111 based laboratory data provides subsurface measurements on the order of inch/cm (core scale)
112 whereas well logs measure up to m/km (reservoir scale) with better resolution for subsurface
113 characterization. The primary goal of this study is to predict and provide permeability changes at
114 the well log scale for the purpose of optimum reservoir quality assessment for CO₂ storage.

115 The local and regional implications of the depth-dependent permeability changes for safe CO₂
116 storage, as this concerns the potential for pore pressure build up, fault reactivation, and induced
117 seismicity, is the second issue of interest. Given the relative proximity of the Norris Lightsey
118 well to the Summerville seismogenic zone of South Carolina, the decision to drill and store CO₂
119 will also need to address questions about environmental safety as follows. Could CO₂ storage in
120 the confined red beds lead to reservoir overpressure capable of causing leakage or threatening the
121 integrity of the storage reservoirs and overlying seals? How can site-specific permeability
122 conditions curtail or expose the risk of fault reactivation and induced seismicity with injection
123 and storage?

114 **Methodology**

115 The approach utilized involves applications of the modified Kozeny-Carman relation (Gomez, et
116 al., 2010, and Mavko et al., 2003) and the Flow Zone Indicator (FZI) technique developed by
117 Amaefule et al. (1993). The modified Kozeny-Carman relation described below in equation 1

118 computes permeability k from porosity ϕ for a rock with predetermined pore space and
 119 geometrical properties.

$$120 \quad k = \left(\frac{d_{Mean}^2}{72\tau^2} \right) \frac{(\phi - \phi_p)^3}{[1 - (\phi - \phi_p)]^2} \quad (1)$$

121 where d_{Mean} is the mean grain size; τ is tortuosity, ϕ is the total porosity and ϕ_p is the percolation
 122 porosity. These properties can be obtained from laboratory measurements on rock samples.
 123 Percolation porosity is the porosity when the pore is disconnected and does not contribute to
 124 flow. It is generally between 1 to 3% (Gomez, et al., 2010, and Mavko et al., 2003). Further
 125 discussion on the Kozeny-Carman relation including its derivation can be found in Mavko et al
 126 (2003), and Schon, (2011).

127 The FZI as used in this study and previous research by Alam et al. (2011), and Prasad (2003)
 128 adapts and extends the Kozeny-Carman relation to enable better characterization of the spatial
 129 distribution of permeability in a reservoir characterized by presence of heterogeneities. It allows
 130 for an assessment of the petrophysical response and sensitivity to dynamic and depth dependent
 131 reservoir changes in a way similar to the applications of geophysical well logs for reservoir
 132 characterization. Its relationship to porosity ϕ and permeability k , which represents the
 133 application to this study, can be seen in the below equation 2.

$$134 \quad FZI = \frac{0.0314}{\epsilon} \sqrt{\frac{k}{\phi}} \quad (2)$$

135 In the above equation, 0.0314 is a constant that accounts for the pore size, tortuosity, pore shape,
 136 and the pore throat to pore-body ratio (Prasad, 2003). ϵ (equation 3) is the ratio of the pore
 137 volume to grain volume.

$$138 \quad \epsilon = \frac{\phi}{1 - \phi} \quad (3)$$

139 Further discussion and derivation of this equation can be found in Schon (2011), Prasad (2003)
140 and Amaefule et al. (1993). The application to a porous reservoir is based on the premise that
141 reservoir units with FZI values within a narrow range belong to one hydraulic unit. The
142 implication of this is that these have similar pore throats and therefore constitute a flow unit. The
143 step-by-step procedure for the implementation of the Kozeny Carman and the FZI technique to
144 predict and provide depth-varying permeability changes in the heterogeneous red beds reservoir
145 are discussed as follows.

- 146 1. Development of a porosity-permeability transform for the study area based on the
147 Kozeny-Carman approach.
- 148 2. Development of FZI from the core derived laboratory measurements in Table 1 to allow
149 for red beds with similar pore throats to be grouped as a single flow unit.
- 150 3. The use of the porosity-permeability relationship in step 1 to convert the porosity from
151 the Norris Lightsey #1 well to reservoir scale permeability at target depths for potential
152 CO₂ injection.
- 153 4. Incorporation of the results from step 3 into equation 2 using the computed FZI values
154 from step 2 to produce the permeability log.

155 In both the Kozeny-Carman and FZI applications for this study, we utilized the existing well
156 data, and the core laboratory measurements for the Norris Lightsey #1 well and other locations
157 with penetrations of the South Georgia Rift red beds (Table 1). The Norris Lightsey #1 well has
158 the deepest penetration of the red beds, covering a depth greater than 800 m below the surface to
159 maintain supercritical CO₂ injection (Akintunde et al., 2013a). The variations in the porosity and
160 permeability data from these locations are due to the influence of depositional environments
161 (Akintunde et al., 2013b). In addition, these study locations share similar lithologic composition,

162 age, geologic history and tectonic setting with red beds recovered from several wells within the
163 basin (Heffner et al., 2012; Chowns and Williams, 1983; Gohn, 1983; and Marine and Siple,
164 1974).

165 **Results**

166 The permeability-porosity relationships based on linear correlation and the Kozeny-Carman
167 relation are shown in Figure 3. A grain size of 250 μm was used based on relevant information
168 from literature review (Mavko et al., 2003, and Gomez et al., 2010), and the subsequent testing
169 and comparison with the direct correlation approach (Figure 3). The Kozeny-Carman porosity-
170 permeability relationship yields a more accurate prediction of permeability from porosity than
171 the linear correlation approach (Figure 3). The Kozeny-Carman relationship takes into account
172 the grain size and tortuosity of the rock, whereas the direct correlation does not account. The FZI
173 adapts and extends the predicted permeability from Kozeny Carman to provide estimates of
174 permeability within definable flow units within the reservoir.

175 The FZI allows for a division of the core-derived porosity and permeability data into flow zone
176 units (Figure 4). It performs this by treating the assigned porosity and permeability contributing
177 to the same flow unit as one FZI value. The consequence of this is that reservoir units with FZI
178 values within a narrow range have similar pore throats and therefore constitute a single hydraulic
179 or flow unit. The distribution of the FZI shows that a large concentration of the data falls within
180 FZI of 0.35. Plugging this value into equation 2 and substituting the well log derived porosity
181 values into the derived porosity-permeability transform (in Figure 3) allow for the production of
182 the permeability log in Figure 5. The permeability log signatures are consistent with the trends
183 exhibited by the porosity log as should be expected given the contribution from porosity. This

184 provides a measure of the reliability of the Kozeny-Carman prediction and the computed FZI
185 values that contributed to the production of the permeability log. It also shows that rock's
186 volumetric properties, such as pore space and grain size distribution that are primarily
187 responsible for porosity, do exert control on permeability. It is remarkable to note that while the
188 porosities are high, the permeability values are low. This is significant as it shows that factors
189 responsible for porosity such as pore size and grain size distribution are not the sole and most
190 dominant controls on permeability. Permeability also depend on the rock's geometrical and fluid
191 flow properties, such as tortuosity, pore shape and pore throats, that are of critical importance to
192 reservoir injectivity.

193 **Discussion**

194 The derived permeability log (Figure 5) manifests the following characteristics: (1) uniform and
195 non-uniform distribution with depths (2) noticeable spikes or increases at depth intervals 1395 to
196 1440 m, 1438 to 1445 m, and 1458 to 1465 m, (3) generally low permeability values that are less
197 than 2 mD , and (4) vertical distribution which is consistent with the trends of the porosity log .

198 The correlation of the permeability log with the porosity and resistivity logs allows for easy
199 recognition of the highly resistive and non-porous diabase sills at 1410 to 1424 m. Within the
200 confined and heterogeneous red beds that are both above and below the impermeable diabase
201 sills (Figures 2 and 5), non-uniform permeability distribution are observed. We interpret the
202 permeability variations with depth to be due to geologic changes and the presence of fluids in the
203 red beds. These geologic changes involve key controls on permeability such as sorting, pore
204 shape, pore throats and tortuosity. Analysis of photomicrographs (Figures 6 to 9) of thin sections
205 on red bed cores recovered from the Rizer #1 Test Borehole in Collenton County, South
206 Carolina, provides evidence for these geologic changes. The Rizer #1 borehole, drilled in spring

207 2012, is within 5 km to the Norris Lightsey well (Figure 1). The similarities in depositional
208 environment and lithologic composition of the Rizer #1 well red beds with the Norris Lightsey
209 lacustrine red beds provide the basis for the use of these thin sections. Analysis reveals cemented
210 and lithified red beds with abundant quartz overgrowths and calcite cement (Figures 6 to 9). The
211 exposure to increased compaction and possibly periods of sustained subsidence during sediments
212 deposition has significantly altered reservoir properties responsible for permeability judging by
213 the presence of clasts and small pore sizes and pore throats seen in the thin sections. These
214 photomicrographs also show irregular pore shapes and sizes in the tectonically deformed red
215 beds which may be responsible for the non-uniform distribution of permeability with depths
216 (Figure 5).

217 The low resistivity in the red bed units is indicative of water or brine saturated red beds. This is
218 because the observed log resistivity values ranging from as low as 0.05 to less than 100 ohm m
219 fall within the range of known resistivity values for water and saltwater reported in Telford et al.,
220 2001. Chemical analysis conducted by Marine and Siple (1974) on pore water from a Dunbarton
221 well with penetration of the red beds found dissolved solid content of approximately 11,000
222 mg/L that supports the interpretation of brine-saturated red beds. Their study also revealed much
223 higher chloride in the red beds (6720 mg/L) in comparison with water from the Cretaceous-
224 Cenozoic coastal plain sediments (1.5 mg/L) and the crystalline metamorphic rock (1260–
225 1400mg/L). Also, there is no gas in the red beds as this would have caused an increase in
226 resistivity. On the other hand, the overlying and non-porous diabase sills are completely dry.
227 This explains the virtually non-existent permeability and the unusually high resistivity of the
228 sills. The interpretation of a brine saturated reservoir is consistent with the plan for a deep saline
229 CO₂ storage system for the South Georgia Rift basin.

230 The consistency in the observed trends of the porosity and permeability logs provides validation
231 for the reliability of the derived permeability log. Their disproportionate values relative to each
232 other however show that the key controls responsible for both are not mutually identical.
233 Porosity is primarily a function of the pore space in a rock. On the other hand, permeability is a
234 function of the pore space and fluid flow properties of the rock such as tortuosity, pore shape and
235 pore throat that control injectivity. This strengthens the need for a permeability log to
236 supplement and complement the porosity log for comprehensive assessment of the suitability of
237 the SGR red beds for CO₂ storage. The correlation with the resistivity log which allows and
238 supports the delineation of the diabase sills and the fully water saturated red beds from the
239 interpretation of the observed permeability distribution also provides an additional, independent
240 verification of the genuineness of the permeability log.

241 The ensuing question from the signatures of the resistivity and permeability logs is what does
242 this mean about the state of the reservoir? The resistivity of a formation based on Archie (1942)
243 varies with porosity depending on the nature and degree of fluid saturation as well as on the
244 rock's cementation and tortuosity. For a fully brine saturated reservoir exhibiting the kind of
245 depth varying porosities shown in Figure 5, the consistently low resistivity also suggests a tightly
246 cemented, compacted rock. This is because the presence of brine (as indicated by the low
247 resistivity) exposes the red beds to chemical dissolution and geochemical reactions that
248 contribute to their cementation and compaction. And with increasing confining stress from burial
249 depths, compaction is further aided. The thin sections (Figures 6 to 9) support the inference for a
250 tightly cemented, compacted rock.

251 The process of compaction or lithification in a reservoir closes pores and/or restricts the
252 interconnectivity between pores that are responsible for permeability (Figures 6 to 9). This

253 process is further enhanced by exposure to increased confining stress with depths. The effect of
254 increasing confining stress is to reduce or weaken the pore pressure by closing openings in a rock
255 responsible for fluid movement (permeability). The thin sections (Figures 6 to 9) support this
256 view as they show severe degradation in grain size distribution, pore sizes and shapes with
257 increasing depths and net confining stress. Apart from geologic changes in the reservoir, the
258 reservoir response to the permeability log signatures may be stress induced. Burial depth, age,
259 geologic history, and composition are additional factors that influence low permeability. The
260 regional implication of the low permeability is that the South Georgia Rift red beds and possibly
261 the ones encountered in other buried Triassic-Jurassic basins in the Southeastern United States
262 are most likely to be low permeable rocks in view of the similarities in age, geologic history and
263 composition (Akintunde et al., 2013b, Marine, 1974, Marine and Siple, 1974).

264 **Applications to CO₂ Storage and Regional Tectonics**

265 In assessing the implications for CO₂ storage, we ask these questions. What does the low
266 permeability mean for reservoir quality determination? How would this affect subsurface
267 suitability for CO₂ storage? How would this impact CO₂ migration and containment in the red
268 beds? Hydrogeologically, the injection, movement and storage of fluids are most effective in
269 underground formations with high porosity and permeability. The direct consequence for low
270 permeability is a reduction in fluid flow and movement even if the porosity or pore space
271 distribution favors substantial fluid storage. Low permeability would impact the degree and
272 effectiveness of injectivity for CO₂ sequestration in the porous formation. Whether or not a
273 reservoir would be viable for long term CO₂ storage depends not only on the storage capacity but
274 also on the quality of reservoir injectivity. A preliminary petrophysical investigation by
275 Akintunde et al., 2013 b demonstrates that the confined South Georgia Rift red beds in the Norris

276 Lightsey do exhibit porous intervals with the potential for substantial CO₂ storage capacity that
277 far exceeds the 30 million tons set by the Department of Energy. Also, a preliminary reservoir
278 modeling of CO₂ injection in the Norris Lightsey red beds by Brantley et al., 2015 basins
279 demonstrates feasibility for injection of at least 30 million tons of CO₂ at a rate of 1 million tons
280 per year for 30 yr. The overarching issue for the kind of subsurface distribution depicted by the
281 permeability log in figure 5 is the impact on the degree of reservoir injectivity. The desirability
282 for an effective CO₂ storage is to have sufficient injectivity to allow seamless fluid flow,
283 movement, and containment without any fear of reservoir failure should the pore pressure
284 exceeds the reservoir capacity. Conceptually, low permeability suggests reduced injectivity
285 which in turn would impact the effectiveness of fluid flow and movement in the heterogeneous,
286 porous red beds. Ideally, an increase in fluid flow and concentration will increase the pore
287 pressure. The implication of increasing pore pressure with fluid injection is to counteract the
288 effect of increased confining stress thereby opening pores and interconnectivity that could
289 enhance permeability or fluid movement. Unless the pre-injection permeability can be physically
290 or geo-mechanically enhanced, the predictably low injectivity will not be promising for effective
291 fluid flow and storage.

292 Low permeability may help with safety and security of storage since the chances of sudden and
293 unsafe pore pressure build up capable of either triggering induced seismicity or threatening the
294 caprock integrity are unlikely with low injectivity. We understand from Zoback and Gorelick
295 (2012) that increasing pore pressure with CO₂ especially in the vicinity of preexisting potentially
296 active faults and considering the critically stressed nature of the crust were likely to increase the
297 potentials for earthquake triggering. It is also inferred from Brantley et al., 2016 that the presence
298 of an active fault with a permeability as low as 1 mD can cause significant CO₂ leakage. With a

309 properly planned injection that incorporates and implements the applicable geological framework
300 as well as robust monitoring and management techniques, the risks of faulting and induced
301 seismicity can be mitigated. A study by Talwani et al. (2007) showing related seimogenic
302 permeability values that are unlikely to cause induced seismicity with fluid injection also lends
303 credence to the potential for safe storage in the low permeable SGR red beds. Ideally, CO₂
304 injection will increase the pore pressure leading to opening of closed pores. So long as this
305 effectively balances the effect of increasing confining stress with depths and does not alter the
306 differential stress equilibrium, the chances of unsafe seismicity within and around the injection
307 reservoir are very unlikely. Moreover, the confining nature of the red beds together with the
308 presence of the impermeable diabase caprocks would ensure containment of the injected CO₂.

309 With adequate pore pressure monitoring before, during, and after injection, the risks to safe CO₂
310 storage may be quickly detected and averted. 4D seismic monitoring can help with understanding
311 and quantifying dynamic reservoir changes to assess storage efficiency as well as the integrity of
312 the overlying cap rocks. The current permeability log would provide the baseline information
313 necessary for the next steps involving reservoir modeling and simulations, seismic modeling, and
314 imaging, as well as field testing to assess the impacts of enhanced permeability on long term
315 storage, the integrity of the overlying diabase sills, and monitor the efficiency and safety of
316 injection and storage.

317 In terms of the application to regional tectonics, the predicted low permeability at depth reflects a
318 compacted, deformed basin with a history of uplift and erosion. The thin sections' analysis on
319 recovered red beds from the Rizer #1 Test Borehole in Collenton County, South Carolina
320 (figures 6 to 9) supports this observation. The interpretation of these photomicrographs reveals
321 the presence of red beds whose physical properties including key controls on permeability such

322 as sorting, pore shape, pore throats and tortuosity have been altered, impacted by tectonically
323 induced post depositional processes (such as compaction and uplift) that have re-shaped the
324 tectonic evolution of the SGR basin following the major phase of rifting. Whether or not the
325 permeability can be recovered and/or enhanced by a physical or geo-mechanical means is
326 beyond the scope of this current research.

327 **Conclusions**

328 The decision to drill and store CO₂ will depend on the quality of the reservoir and the safety of
329 injection and containment. Of importance to reservoir quality are the in-situ porosity and
330 permeability that determine the storage capacity and injectivity. Knowledge of the permeability
331 regime is an extremely valuable rock property that dictates and determines the progress and
332 efficiency of injection and storage. Its correlation and interpretation with porosity and resistivity
333 logs to better understand and characterize the state of the red beds reservoir for CO₂ storage
334 provides the motivation for this study. Permeability is most relevant for correlation with these
335 logs, because of its strong connection to fluid saturation, grain size, pore shapes, cementation and
336 tortuosity that are key controls on porosity and resistivity. Core based laboratory data do not
337 have the resolution, scale, and continuity required for correlation and interpretation with well
338 logs. Consequently, a significant, new contribution from this work is the development of a
339 permeability log for the study area based on a robust methodology involving applications of the
340 Kozeny-Carman relation and the Flow Zone Indicator technique. The rationale for the use of
341 these two approaches was to ensure reliable permeability prediction and distribution that
342 considers the pore space and geometrical properties of the target red beds. The development of
343 this permeability log offers an alternative way to save time and significant cost associated with
344 expensive well drilling and logging for in situ permeability measurements for reservoir

345 characterization. It would also aid dynamic reservoir modeling of the distribution of fluid flow to
346 better characterize the CO₂ injection distribution and efficiency for the purpose of storage
347 optimization and management.

348 The interpretation of the permeability log supported by the correlation with the porosity and
349 resistivity logs shows non-uniform distribution with depths possibly caused by geological and
350 stress induced changes in the heterogeneous red beds. Moreover, the petrophysical responses in
351 both the resistivity and permeability logs are generally low. We interpret this in conjunction with
352 the porosity distribution to suggest: (1) the South Georgia Rift is a tightly cemented and
353 compacted reservoir, and (2) a reservoir exposed to increased confining stress. Increasing
354 confining stress closes and/or restricts reservoir openings responsible for porosity and
355 permeability. On the other hand, increasing pore pressure with CO₂ injection has the potential to
356 counteract the effects of increased confining stress by opening closed pores or enhancing weak
357 pores for efficient fluid movement and storage over time. However, low permeability will reduce
358 injectivity that is a key requirement for the efficiency of CO₂ injection and storage. We also
359 conclude that the predicted low permeability distribution with depth is a function of the active
360 and passive post-tectonic depositional processes that have impacted the physical properties of the
361 Triassic red beds.

362 **References Cited**

- 363 Akintunde, O.M., C.C. Knapp, J.H. Knapp, and D.M. Heffner, 2013a, New constraints on buried
364 Triassic basins and regional implications for subsurface CO₂ storage from the SeisData6 seismic
365 profile across the Southeast Georgia coastal plain: *Environmental Geosciences*, v.20, p. 17-29.
- 366 Akintunde O.M., C.C. Knapp, and J.H. Knapp, 2013b, Petrophysical characterization of the
367 South Georgia Rift basin for supercritical CO₂ storage: a preliminary assessment: *Environmental*
368 *Earth Science* v. 70, p. 2971-2985.

369 Alam, M.M., I.L. Fabricius, and M. Prasad, 2011, Permeability prediction in chalks: American
370 Association of Petroleum Geologists Bulletin, v. 95, p.1991-2014.

371 Amaefule, J.O., M. Altunbay, D. Tiab, D.G. Kersey, and D.K. Keelan, 1993, Enhanced reservoir
372 description: Using core and log data to identify hydraulic (flow) units and predict permeability in
373 uncored intervals/wells: Society of Petroleum Engineers Paper v. 26436, p. 1-16.

374 Archie, G.E., 1942, The electrical resistivity log as an aid in determining some reservoir
375 characteristics : Transactions of the American Institute of Mining, Metallurgical, and Petroleum
376 Engineers, v.146, p. 54-62.

377 Brantley, D., M. Waddell, J. Shafer and V. Lakshmi, 2016, Inclusion of Faults in 3-D Numerical
378 Simulation of Carbon Dioxide Injection into the South Georgia Rift Basin, South Carolina:
379 International Journal of Earth Science and Geophysics, v. 2, p. 1-11

380 Brantley, D., J. Shafer and V. Lakshmi, 2015, CO₂ injection simulation into the South Georgia
381 Rift Basin for geologic storage: A preliminary assessment: Environmental Geosciences, v. 22,
382 pp. 1-18

383 Chowns, T. M., and C. T. Williams, 1983, Pre-Cretaceous rocks beneath the Georgia coastal
384 plain: Regional implications, in G. S. Gohn, ed., Studies related to the Charleston, South
385 Carolina, earthquake of 1886: Tectonics and seismicity: U.S. Geological Survey Professional
386 Paper 1313, p. L1–L42.

387 Gohn, G. S., 1983, Geology of the basement rocks near Charleston, South Carolina: Data from
388 detrital rock fragments in lower Mesozoic(?) rocks in Clubhouse Crossroads test hole #3, in G.
389 S. Gohn, ed., Studies related to the Charleston, South Carolina, earthquake of 1886: Tectonics
390 and seismicity: U.S. Geological Survey Professional Paper 1313, p. E1–E22.

391 Gohn, G. S., B. B. Houser, and R. R. Schneider, 1983, Geology of the lower Mesozoic(?)
392 sedimentary rocks in Clubhouse Crossroads test hole #3 near Charleston, South Carolina, in G.
393 S. Gohn, ed., Studies related to the Charleston, South Carolina, earthquake of 1886: Tectonics
394 and seismicity: U.S. Geological Survey Professional Paper 1313, p. D1–D17.

395 Gomez, T.C., J. Dvorkin, and T. Vanorio, 2010, Laboratory measurements of porosity,
396 permeability, resistivity, and velocity on Fontainebleau sandstones: Geophysics, v. 75, p. E191-
397 E204.

398 Heffner, D.M., J.H. Knapp, J.H. O.M. Akintunde, and C.C. Knapp, 2012, Preserved extent of
399 Jurassic flood basalt in the South Georgia Rift: A new interpretation of the J horizon: Geology,
400 v.40, p. 167-170.

401 Marine, W., 1974, Geohydrology of buried Triassic basin at Savannah River Plant, South
402 Carolina: American Association of Petroleum Geologists Bulletin, v.58, p. 1825-1837.

403 Marine W., and G.E. Siple, 1974, Buried Triassic basin in the central Savannah River area:
404 Journal of Geological Society of American Bulletin. v. 85, p. 311–320.

405 Mavko, G., T. Mukerji, and J. Dvorkin, 2003, The Rock Physics Handbook - Tools for seismic
406 analysis in porous media: Cambridge, Cambridge University Press, 329 p.

407 McBride, J.H., K.D. Nelson, and L.D. Brown, 1989, Evidence and implications of an extensive
408 early Mesozoic rift basin and basalt/diabase sequence beneath the southeast coastal plain:
409 Geological Society of America Bulletin, v. 101, p. 512-520.

410 Olsen, P.E., A.J. Froelich, D.L. Daniels, J.P. Smooth, and J.W. Gore, 1991, Rift basins of early
411 Mesozoic age: Geology of the Carolinas, Carolina Geological Society 50th Anniversary,
412 Volume, Ed Horton, p. W 142-170.

413 Prasad, M, 2003, Velocity-permeability relations within hydraulic units: Geophysics v. 68,
414 p.108–117.

415 Schon, J.H., 2011, Physical Properties of Rocks: Amsterdam, Elsevier, 350 p.

416 Talwani, P., L. Chen, and K. Gahalaut, 2007, Seismogenic Permeability, ks: Journal of
417 Geophysical Research 112, B07309, doi:10.1029/2006JB004665.

418 Telford, W.M., L.P. Geldart, and R.E. Sheriff, 2001, Applied Geophysics: Cambridge,
419 Cambridge University Press, 770 p.

420 Weatherford Laboratories Reports, 2014, Geologic Characterization of the South Georgia Rift
421 basin for source proximal CO2 storage based on analysis of samples from Rizer #1 test borehole
422 Colleton County, South Carolina, and the United States Geological Survey Clubhouse
423 Crossroads test hole no. 3, Dorchester County, South Carolina, 149 p.

424 Zoback, M.D., and S.M. Gorelick, 2012, Earthquake triggering and large-scale geologic storage
425 of carbon dioxide: Proceedings of the National Academy of Sciences of the United States of
426 America, v. 109, p. 10164-10168.

427

Figures

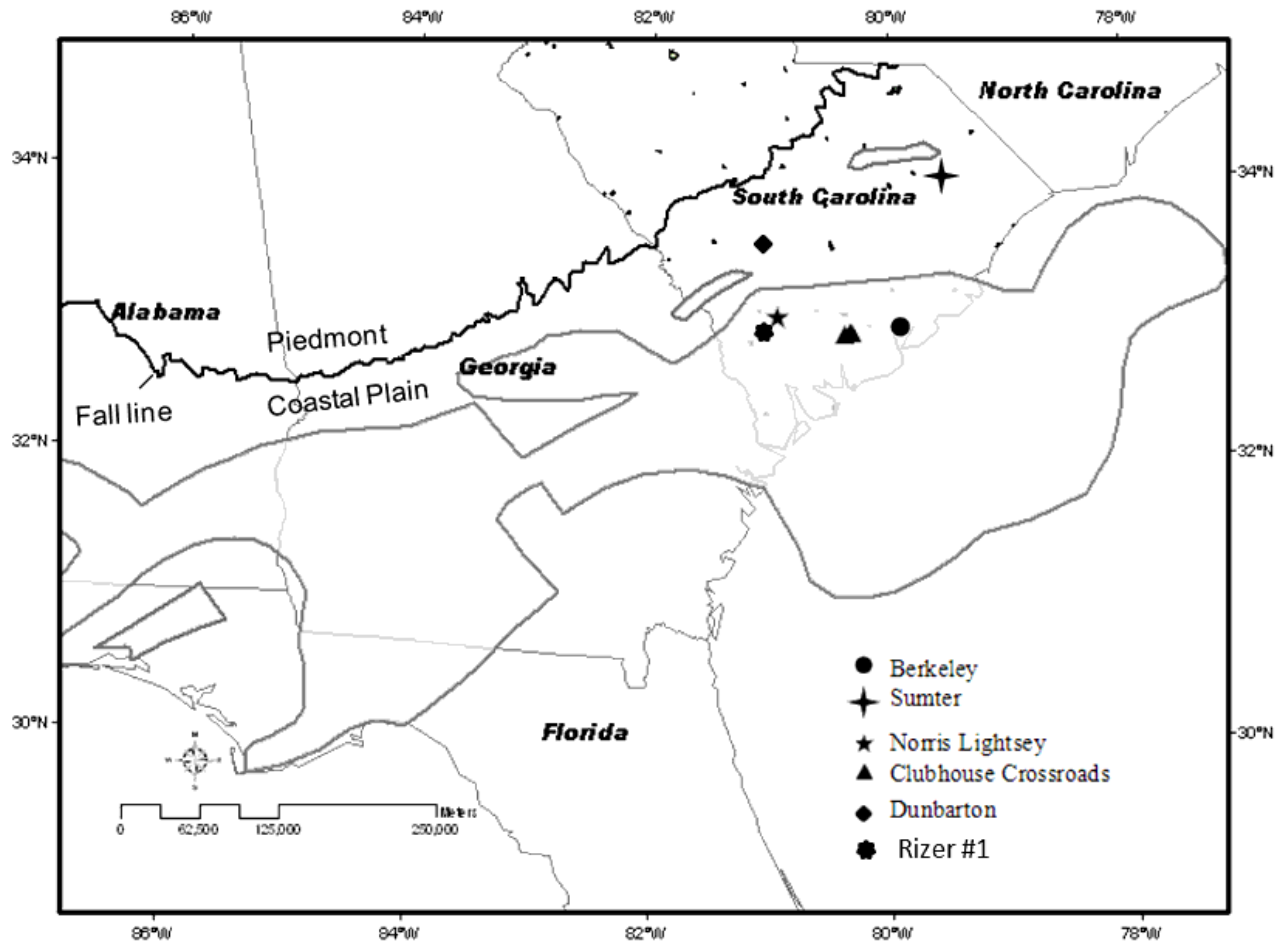


Figure 1

Areal extent of the South Georgia Rift basin (modified from Chowns and Williams, 1983) showing the Norris Lightsey #1 well study location. Other wells used in this study such as Sumter, Berkeley, Clubhouse Crossroad, Dunbarton and newly drilled Rizer #1 are shown. Gray shaded area represents the areal extent of the basin

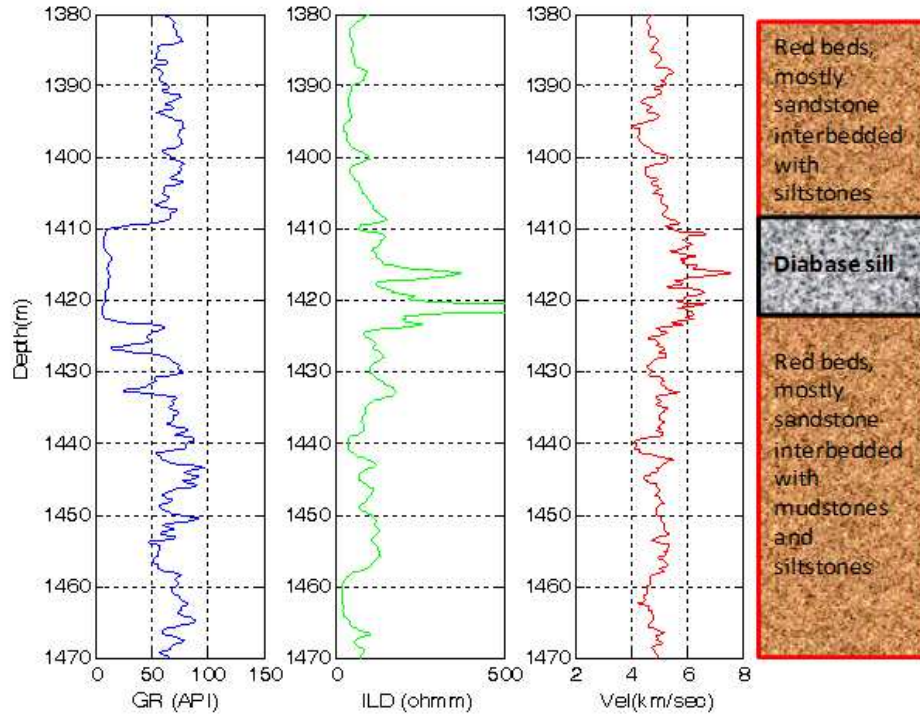


Figure 2

Target reservoir depths from the Norris Lightsey #1 well for potential CO₂ storage. The diabase sill stands out from the red beds by its low Gamma Ray (GR in API), high resistivity (deep induction resistivity log, ILD, in ohm-meter), and high velocity (km/s)

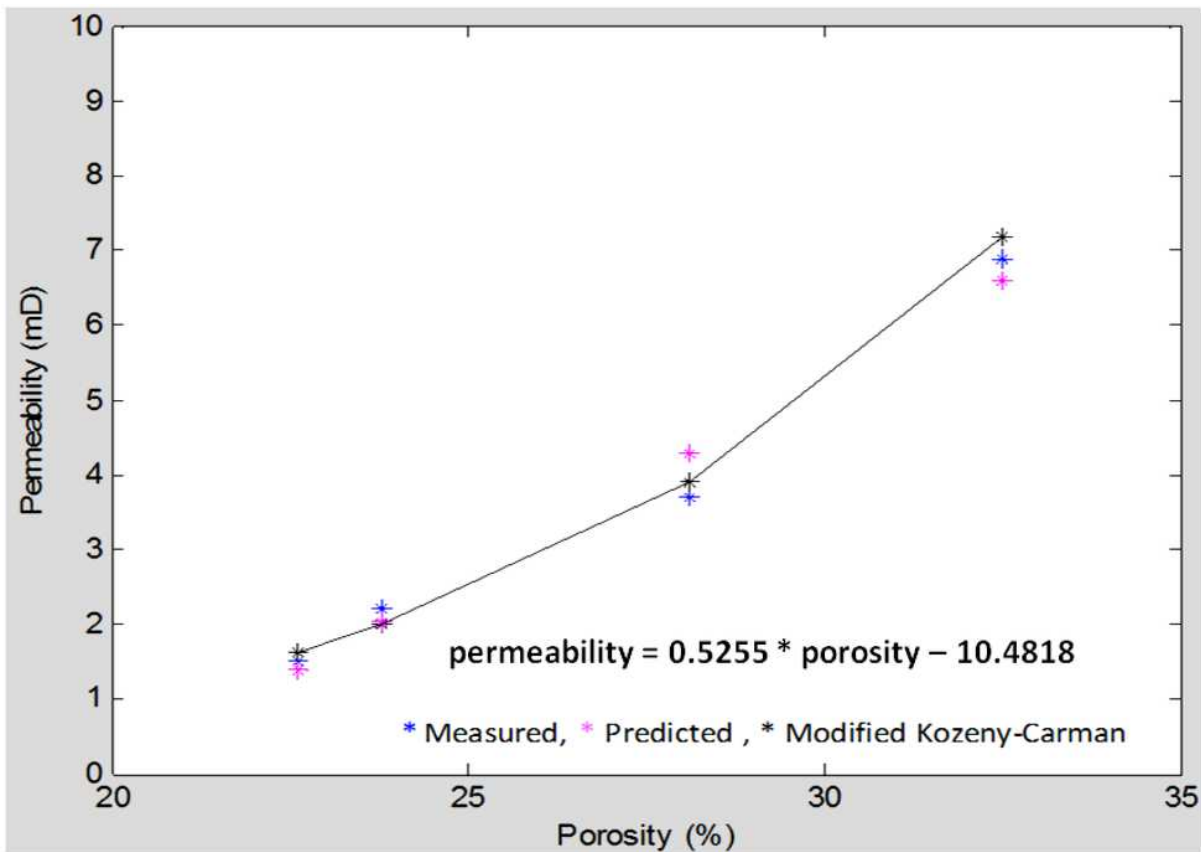


Figure 3

Permeability versus Porosity for the Norris Lightsey #1 well data shown in Table 1. Prediction by Kozeny-Carman relation provided the most reliable fit for the plotted data points.

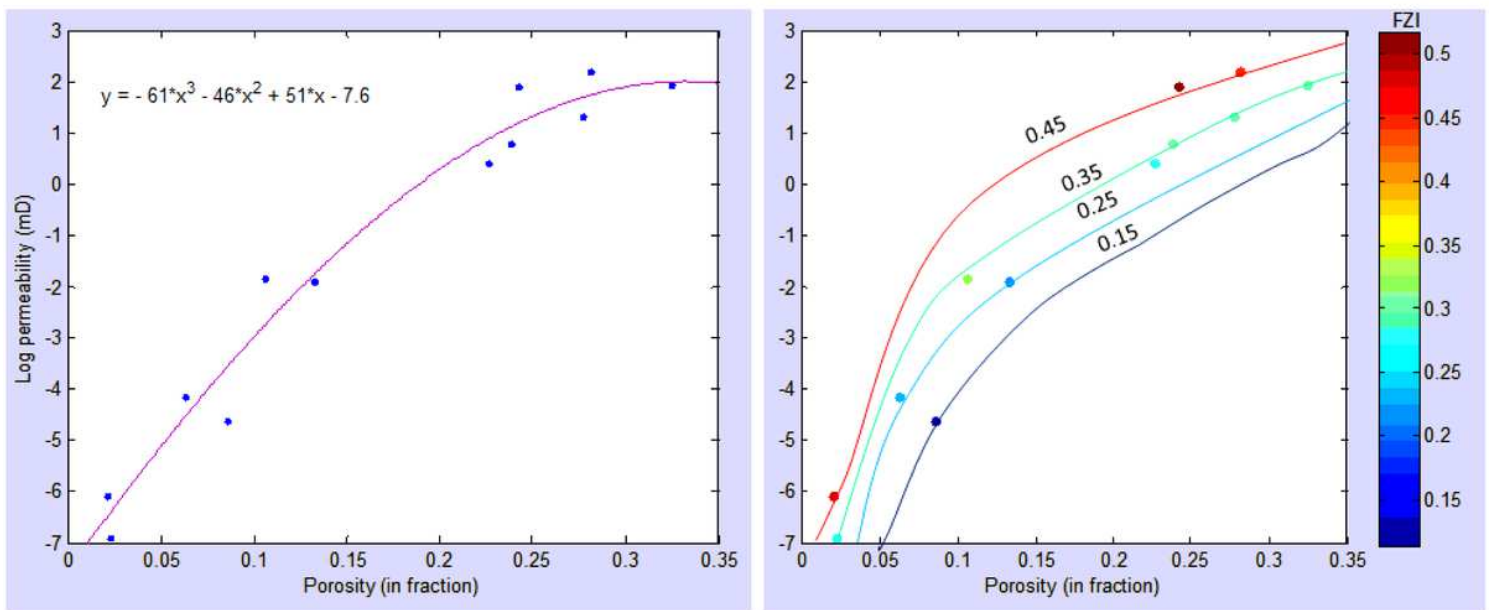


Figure 4

Permeability based on the concept of Flow Zone Units (FZI). The permeability-porosity distribution for well locations shown in Table 1 is plotted on the left. The computed flow zone indicators are shown on the right. The flow zone intervals are shown by different colors in the color bar.

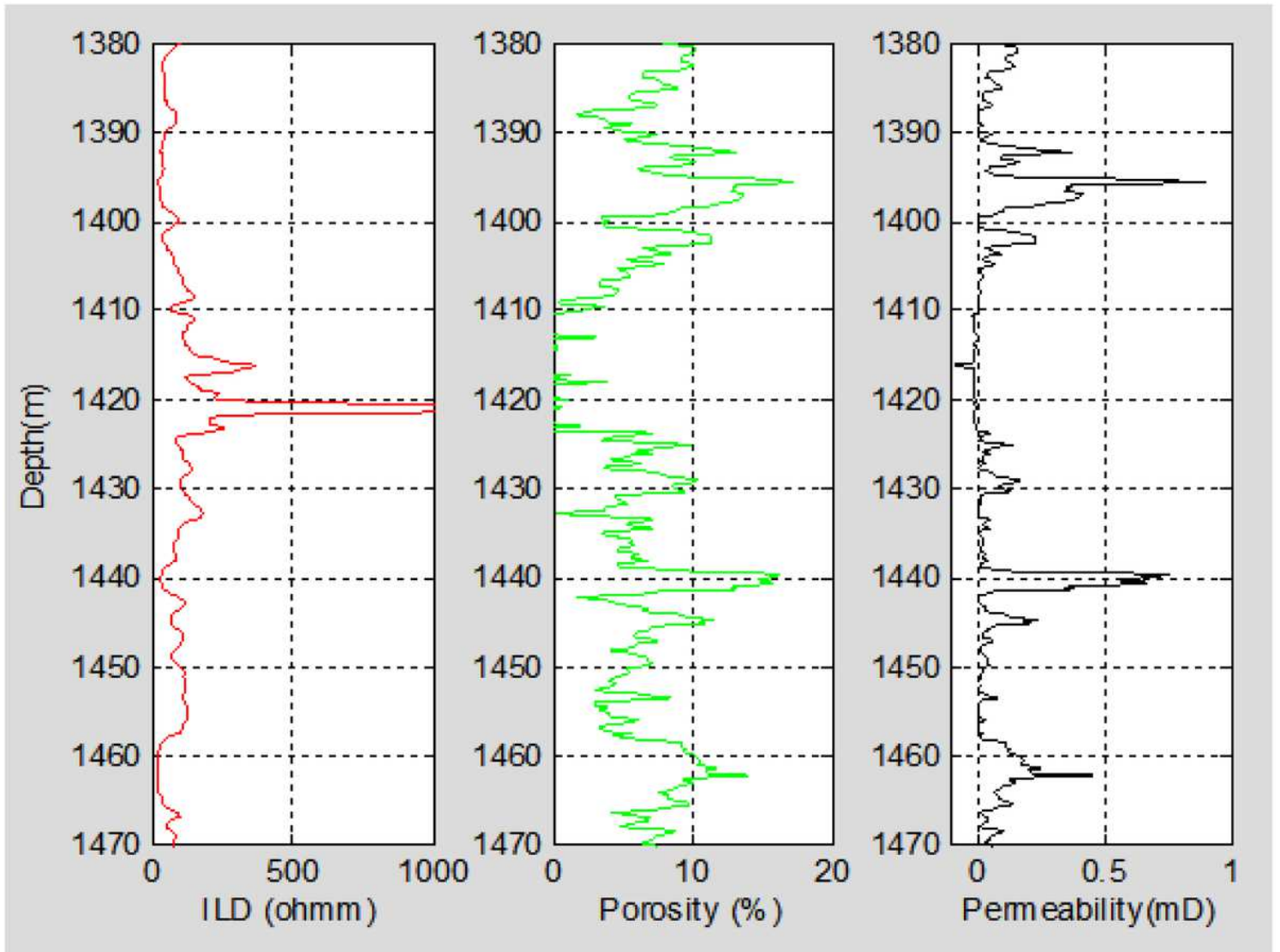


Figure 5

Predicted permeability changes at the reservoir scale using flow zone interval 0.35. The derived permeability follows same trend as the porosity log that is characterized by significant changes in the red beds at 1400, 1440 and 1465 m. Plotted alongside is the deep lateral induction (ILD) resistivity log. The high ILD reading is due to presence of diabase sills.

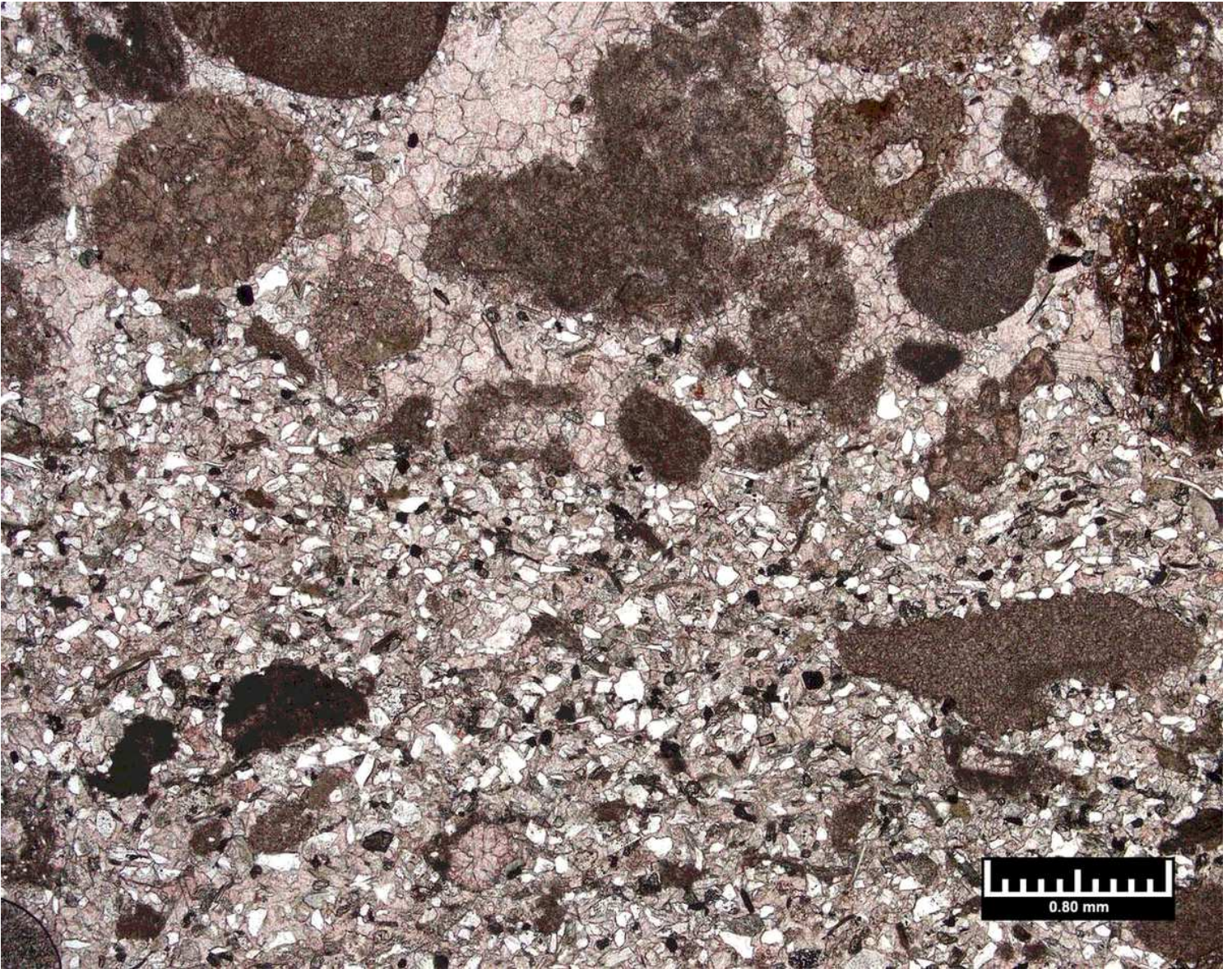


Figure 6

Photomicrograph of a thin section of a red bed at the Rizer #1 Test Borehole at 1172.11 m and net confining stress 11.03 MPa (Megapascal). It consists of very fine-grained sandstone and coarse-grained calcitic and mudstone clasts. Though well sorted, the presence of clasts and compaction are factors that reduce the permeability. The various colors are due to variations in mineralogical composition consisting of quartz and calcite, biotite, feldspar, and chlorite (after Weatherford Laboratories Report, 2014).

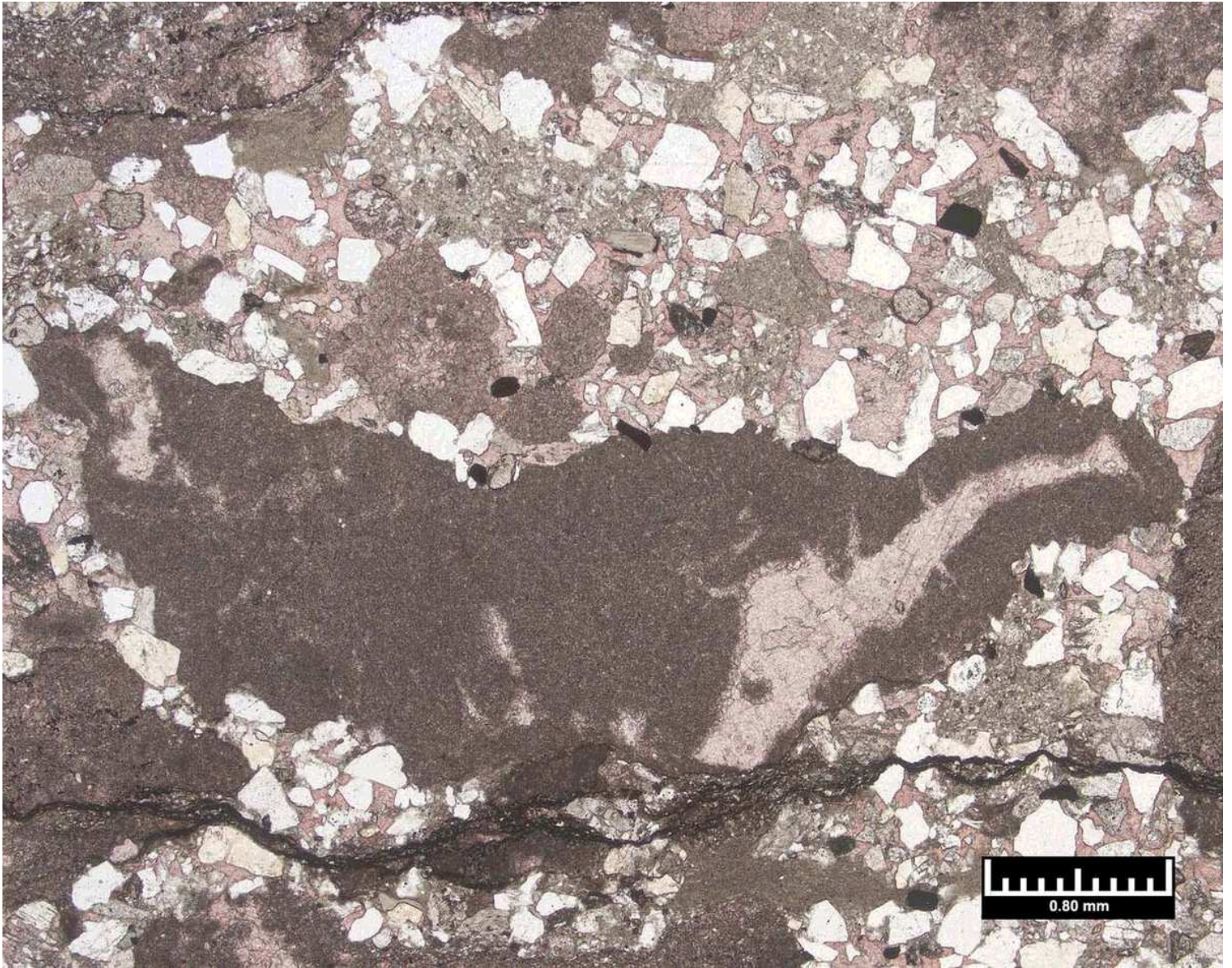


Figure 7

Photomicrograph of a thin section of a medium grained red bed at the Rizer #1 Test Borehole at 1602.64 m and net confining stress 11.38 MPa. It is a poorly sorted, sandy clast conglomerate mixed with silt and clay. The dark color is due presence of claystone and silty claystone casts. The light red color is due to presence of calcite. Quartz grains are common with minor amounts of potassium feldspar (after Weatherford Laboratories Report, 2014).

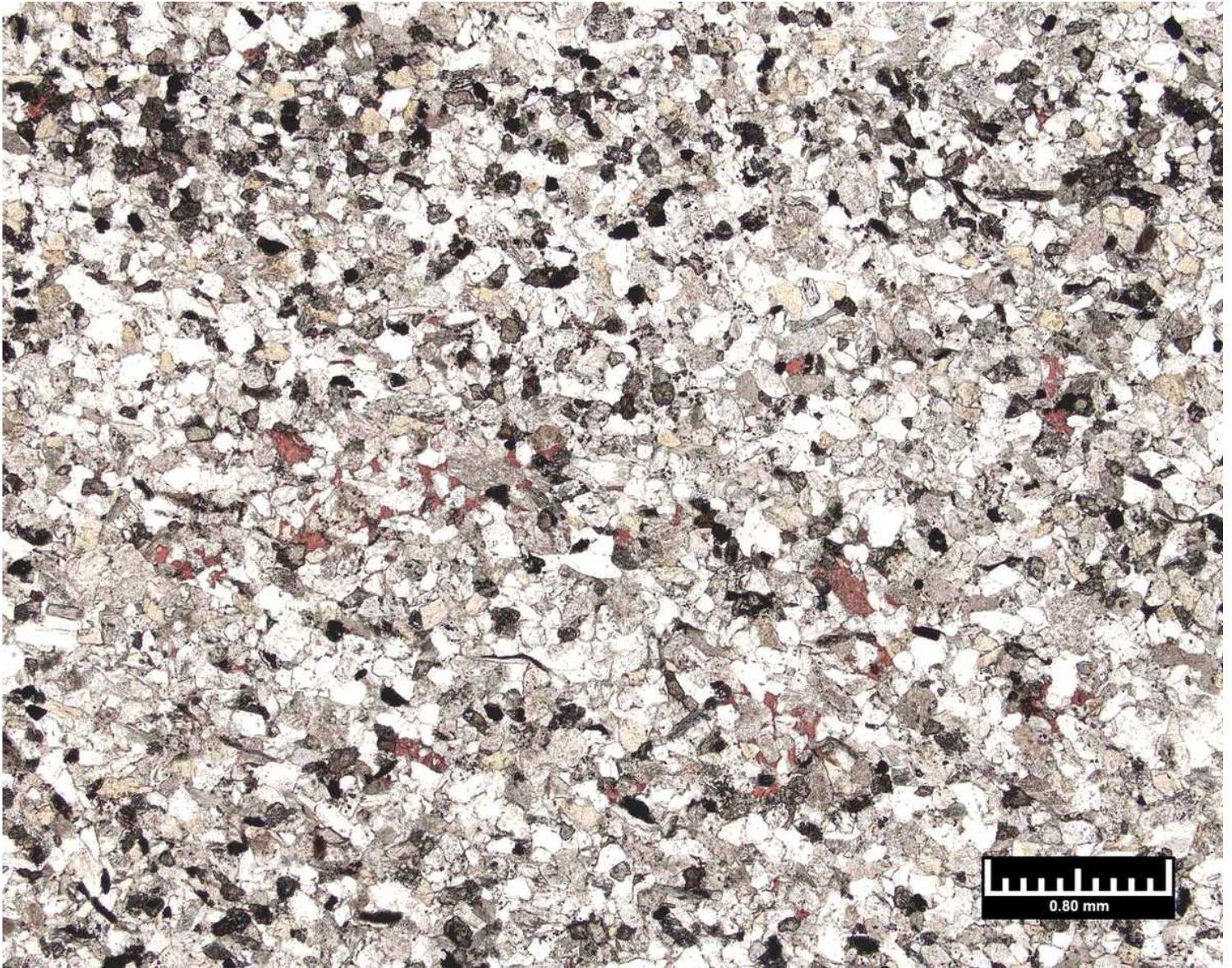


Figure 8

Photomicrograph of a thin section of a finely grained red bed at the Rizer #1 Test Borehole at 1773.48 m, and net confining stress 12.76 MPa. Though well sorted, it is highly compacted and cemented effectively reducing the pore size and pore connectivity responsible for permeability. Quartz and calcite (light red) are common (after Weatherford Laboratories Report, 2014).

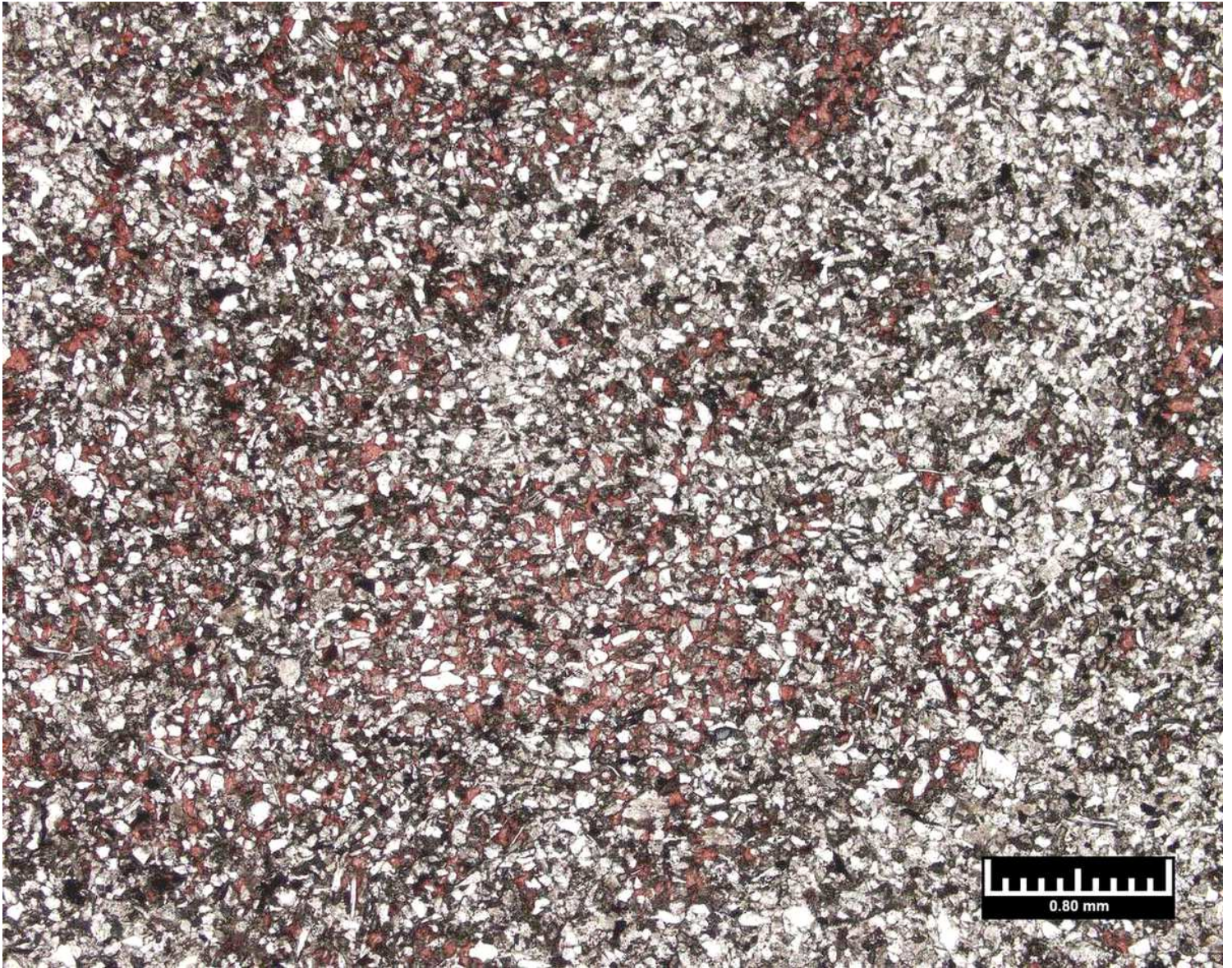


Figure 9

Photomicrograph of a thin section of a very fine grained red bed at the Rizer #1 Test Borehole at 1862.33 m, and net confining stress 13.10 MPa. It is well sorted but its lithified and compacted nature is not helpful to permeability. Changes in color are due to variations in mineralogy (after Weatherford Laboratories Report, 2014).

Supplementary Files

This is a list of supplementary files associated with this preprint. Click to download.

- [Table.pdf](#)